Supporting Information

Atomically Dispersed Nanoenzymes-Based Synergistic Mild Photothermal/Nanocatalytic-Therapy for Eradicating Multidrug-Resistant Bacteria and Accelerating Infected Wound Healing

Ying Qu,[a] Liang Zhuang,[b] Wuren Bao,[a] Chunlin Li,[c] Hongyu Chen,[d] Shan He,[b,*] Hui Yao,[d,*] Quanjin Si[c,*]

[a] College of Nursing, Inner Mongolia Minzu University, Tongliao, Inner Mongolia, 028000, China.

[b] Key Laboratory of Geriatric Nutrition and Health, Ministry of Education, Beijing Technology and Business University, 11 Fucheng Road, Haidian District, Beijing, 100048, P. R. China.

[c] The Third Healthcare Department of The 2th Medical Center, The 2th Medical Center, Chinese PLA General Hospital, Beiing 100853, China.

[d] Pain Department, Eye Hospital China Academy of Chinese Medical Sciences, Beijing, 100040, China.

[*] Corresponding authors.

E-mail addresses: vh30@163.com (S. He); foxyaohui@126.com (H. Yao); quanjin2004@sohu.com (Q. Si).

Experimental Section

Materials. Manganese (II) acetate tetrahydrate (Mn(CH$_3$COO)$_2$•4H$_2$O), Copper (II) acetate monohydrate (Cu(CH$_3$COO)$_2$·H$_2$O), trimesic acid (BTC), hydrogen peroxide (H$_2$O$_2$, 30 wt%), dicyandiamide, 3,3',5,5'-tetramethylbenzidine dihydrochloride hydrate (TMB), 1,3-diphenylisobenzonfuran (DPBF), and carboxylic PEG acid were purchased from Aladdin Biochemical Technology Co., Ltd (Shanghai, China). 2',7'-dichlorofluorescin diacetate (DCFH-DA), SYTO9, propidium iodide (PI), and cell counting kit-8 (CCK-8) were obtained from Beijing Solarbio Science & technology Co., Ltd. (Beijing, China). All of these chemicals were of reagent grade or better, and used without further purification. Deionized (DI) water was obtained by a Milli-Q Water Purification system.

Preparation of Cu/Mn-DSAzymes. The Cu/Mn-BTC MOF precursor was initially synthesized through a chemical precipitation method. In a succinct procedure, a mixture of Cu(CH$_3$COO)$_2$·H$_2$O (0.162 g) and Mn(CH$_3$COO)$_2$·4H$_2$O (0.058 g) was dissolved in a 100 mL ethanol-water solution. Subsequently, 0.116 g of 1,3,5-Benzenetricarboxylic acid was dissolved in another 100 mL ethanol-water solution and added to the above mixture, which was stirred at room temperature for 2 hours. The resulting solid products were separated through centrifugation, thoroughly washed with water, and subsequently dried in a vacuum oven.

Subsequently, 0.1 g of the Cu/Mn-BTC MOF precursor was meticulously blended with dicyandiamide through grinding until a homogeneous mixture was achieved. The resultant blend underwent heating in a tube furnace at 800 °C under N$_2$ flow for 3 hours. Following pyrolysis, the resulting products were washed extensively with ethanol/deionized water and dilute acid under ultrasound, obtaining Cu/Mn-DSAzymes.

Preparation of PEGylated Cu/Mn-DSAzymes. The mPEG-COOH and Cu/Mn-DSAzymes were added into ethanol-water solution, followed by magnetic stirring for homogenization and heating at 60 °C. Then, the obtained products was separated by centrifugation, washed thoroughly with ethanol/water and dried under vacuum oven, giving the final PEGylated Cu/Mn-DSAzymes. To simplify discussion, the PEGylated Cu/Mn-DSAzymes were referred to simply as Cu/Mn-DSAzymes in the text below.

Photothermal effect and photothermal conversion efficiency. The Cu/Mn-DSAzymes solution with various concentrations (0, 40, 80, and 160 μg mL^{-1}) was exposed to 1064

nm laser (1.0 W cm^{-2}) for 10 min, and the temperature variation were monitored by a thermocouple probe to an accuracy of 0.1 °C. The photothermal effect of Cu/Mn-DSAzymes solution (80 μg mL^{-1}) under various laser power density irradiation (0.6, 1.0 and 1.4 W cm^{-2} of 1064 nm laser) was measured in the same way.

The photothermal conversion efficiency (η) was calculated using the following equation (Eqs 1).

$$\eta = \frac{hs(Tmax\text{–}Tamb) - Q^0}{I(1 - 10^{-A\lambda})}$$

Eqs 1

where h was the heat transfer coefficient, s was the surface area of the container, T_{max}–T_{amb} was the temperature change of the solution under continuous irradiation by a 1064 nm laser, Q^0 was the heat input due to light absorption by the solvent, I was the laser density (1.0 W cm^{-2}) and $A\lambda$ was the absorbance at 1064 nm. The value of hs can be calculated using the following equation (Eqs 2).

$$hs = \frac{m_D \times C_D}{\tau_s}$$

Eqs 2

where m_D (1.0 g) and C_D (4.2 J g^{-1}) were the mass and heat capacity, respectively, of the Deionized water dispersion medium. τ_s represented the rate of heat transfer from the solution to the environment, which was calculated using the equation (Eqs 3).

$$\tau_s = -\frac{t}{Ln\theta}$$

Eqs 3

The value of τs was gained by the linear relationship between $-Ln(\theta)$ and time (t) obtained from the cooling period of Cu/Mn-DSAzymes.

Measurement of CAT-like activity. The CAT-like activity of Cu/Mn-DSAzymes was assessed by quantifying oxygen production using a portable dissolved oxygen meter. Specifically, Cu/Mn-DSAzymes at a concentration of 80 μg mL^{-1} was combined with varying concentrations of H_2O_2 (1, 2, and 4 mM) in a PBS solution. Subsequently, the real-time oxygen concentration was recorded over a 10-minute duration.

Furthermore, kinetic assays of Cu/Mn-DSAzymes with H_2O_2 as the substrate were conducted by introducing different concentrations of H_2O_2 solution. For each H_2O_2 concentration, the initial reaction rates (V_0) were determined based on changes in real-

time oxygen concentration. The resulting rates were graphed against H_2O_2 content and subjected to fitting with Michaelis-Menten curves (Eqs 4). This fitting facilitated the determination of the Michaelis-Menten constant (K_m) and maximal reaction velocity (V_{max}), where [S] represented the substrate content.

$$v_0 = \frac{V_{max} \cdot [S]}{K_m + [S]}$$

Eqs 4

Measurement of OXD-like activity. DPBF was employed to ascertain the presence of superoxide radicals ($\cdot O_2^-$). Specifically, a solution containing Cu/Mn-DSAzymes (80 μg mL^{-1}), H_2O_2 (1 mM), and DPBF was introduced into a PBS solution. The production of $\cdot O_2^-$ was quantified by monitoring the reduction in absorbance at 420 nm.

OXD-like kinetic assays of Cu/Mn-DSAzymes with TMB as the substrate were conducted by introducing varying concentrations of TMB solution. For each TMB concentration, the initial reaction rates (V_0) were determined based on absorbance changes using the Beer-Lambert Law (Eqs 5). Subsequently, the rates were graphed against TMB content and subjected to fitting with Michaelis-Menten curves (Eqs 4). Utilizing the Michaelis-Menten model (Eqs 4) facilitated the determination of the Michaelis-Menten constant (K_m) and maximal reaction velocity (V_{max}).

$$A = \varepsilon bc$$

Eqs 5

Characterization. The aberration-corrected high-angle annular dark-field scanning transmission electron microscopy (AC-HAADF-STEM) images were recorded by JEM-ARM300F with a spherical aberration corrector working at 300 kV. Powder X-ray diffraction (XRD) patterns were collected on a Bruker X-ray diffractometer (D8 focus, Cu Kα, λ = 0.15178 nm) operated at a scan rate of 0.1 °/s. XPS measurements used an ESCALAB 250Xi (Thermo Scientific), equipped with a non-monochromatized Al-Kα X-ray source (hv=1486.7 eV). UV-Vis-NIR absorption spectra were obtained on a Shimadzu UV-3600 spectrophotometer. The chemical compositions of prepared samples were determined using a Shimadzu ICPS-7500 inductively coupled plasma–atomic emission spectrometer (ICP−AES). Extended X-ray absorption fine structure (EXAFS) measurements at the Cu/Mn K-edge were performed at the beamline 1W1B of the Beijing Synchrotron Radiation Facility (BSRF), Institute of High Energy

Physics (IHEP), Chinese Academy of Sciences (CAS). The typical energy of the storage ring was 2.5 GeV with a maximum current of 250 mA. The Si (111) double crystal monochromator was used. The IFFEFIT 1.2.11 date analysis package (Athena, Artemis, Atoms, and FEFF6) was used for the date analysis and fitting. Confocal fluorescence images were obtained on a Nikon A1R Eclipse Ti confocal laser scanning microscope fitted with a 40× water immersible objective.

In vitro **antibacterial activity.** The antibacterial efficacy of Cu/Mn-DSAzymes was evaluated using the agar plate dilution method and the growth curve method. In the agar plate dilution approach, MRSA and *E. coli* bacteria were cultured in lysogeny broth medium at 37 °C for 16 hours to attain the logarithmic growth phase. Subsequently, the bacterial solution was treated with PBS + H_2O_2 (0.1 mM), NIR-II + H_2O_2 (0.1 mM), Cu/Mn-DSAzymes, Cu/Mn-DSAzymes + NIR-II, Cu/Mn-DSAzymes + H_2O_2 (0.1 mM), and Cu/Mn-DSAzymes + H_2O_2 (0.1 mM) + NIR-II groups at 37 °C for 4 hours, maintaining an equivalent Cu/Mn-DSAzymes concentration of 80 μg mL^{-1}. In cases involving NIR-II irradiation, the samples were exposed to a 1064 nm laser. The resulting bacterial suspensions were diluted 10,000 times, and 50 μL of the diluted solution was plated onto solid culture medium. These petri dishes were then incubated at 37 °C for 24 hours to observe bacterial growth. The colony-forming units (CFU) of MRSA and *E. coli* were subsequently enumerated. For the growth curve method, suspensions of MRSA and *E. coli* treated with various groups were mixed in LB medium. These different treatment groups were then added to 96-well plates (n=3) and incubated in a fully automated growth curve analyzer (Bioscreen C). The optical density values were monitored at a wavelength of 600 nm (OD600) until the growth curve reached a plateau stage.

SYTO9 and PI double staining was employed to discern live/dead MRSA and *E. coli* bacteria following diverse treatments. Fluorescent images were captured using confocal laser scanning microscopy. For reactive oxygen species (ROS) detection, DCFH-DA was utilized to label MRSA bacteria under distinct treatments, and the fluorescence intensity of DCF reflected the ROS levels. In investigating bacterial morphology, MRSA and *E. coli* bacteria subjected to various treatments were fixed with 2.5% glutaraldehyde for 2 hours at room temperature. Subsequently, the bacteria underwent sequential treatment with ethanol concentrations of 50%, 70%, 80%, 90%, 95%, and 100%. The resulting

bacterial morphology was observed using scanning electron microscopy (SEM).

***In vitro* antibacterial mechanism.** The antibacterial mechanism was elucidated through the assessment of K^+, β-galactosidase, and DNA leakage from MRSA. K^+ levels were measured by incubating MRSA in LB medium at 37 °C for 24 hours, followed by treatment with various groups and subsequent analysis of MRSA suspensions. The concentration of K^+ was determined using sodium tetraphenylboronate. To assess β-galactosidase activity, MRSA was cultured in LB medium at 37 °C for 24 hours. The collected bacteria were subsequently incubated in M9 lactose medium at 37 °C for 8 hours, followed by centrifugation and collection. Bacterial suspensions were mixed with different treatment groups and incubated at 37 °C. The supernatant was collected at intervals, and the optical density of p-nitrophenol was measured at 400 nm using a microplate reader. Concentrations of K^+ and β-galactosidase were calculated based on standard curves. Intra-bacterial DNA levels were determined by measuring OD260 values of the supernatant of bacterial suspensions after diverse treatments. Briefly, MRSA was treated with different groups, incubated at 37 °C, and subsequently, bacterial suspensions were centrifuged, and the absorbance value of the resulting supernatants was read at 260 nm.

Cytotoxicity evaluation. The biocompatibility assay of Cu/Mn-DSAzymes was conducted on L929 cells using a Cell Counting-Kit 8 (CCK-8) assay. Initially, cells were incubated in a 25 cm^2 cell-culture flask and subsequently seeded into a 96-well plate (1×10^4 cells/well) by pipetting. The cell medium was then replaced with fresh medium containing different concentrations of Cu/Mn-DSAzymes (0, 20, 40, 80, and 160 μg mL^{-1}). Following a 24-hour incubation, the cells were washed once with PBS and further incubated with CCK-8 for 1 hour. Moreover, after co-incubation with Cu/Mn-DSAzymes (80 μg mL^{-1}) for 24 hours, 72 hours, and 120 hours, respectively, the L929 cells were double stained with calcein-AM and PI to distinguish live/dead cells. Fluorescent images were obtained using confocal laser scanning microscopy. For the hemocompatibility assay, fresh red blood cells (RBCs) were obtained from mice and diluted with normal saline. The RBC suspensions were then co-incubated with normal saline (negative control), distilled water (positive control), or different concentrations of Cu/Mn-

DSAzymes. The supernatant was subsequently removed by centrifugation, the absorbance was measured at 545 nm, and the hemolysis rate was calculated.

In vivo healing of MRSA-infected wounds. All animal experiments strictly adhered to relevant laws and institutional guidelines of the University of Chinese Academy of Sciences (UCAS) and received approval from the Model Animal Research Center of the Institute of Process Engineering, Chinese Academy of Sciences. Dorsal hair of ICR mice (6 weeks old, female) was shaved, and full-thickness defective skin wounds were created. Following wound formation, MRSA suspension was inoculated at the wound sites. To confirm the success of infection, bacterial samples were collected from the wounds via sterilized cotton swabs at 12 hours post-infection or 9 days post-management. Swabs were placed in 1 mL of normal saline solution, and loads of live MRSA in diluted suspensions were investigated after culturing MRSA on LB agar plates for 24 hours at 37 °C.MRSA-infected ICR mice were randomly divided into five groups (n=5) and treated with PBS + H_2O_2 (0.1 mM), NIR-II + H_2O_2 (0.1 mM), Cu/Mn-DSAzymes, Cu/Mn-DSAzymes + NIR-II, Cu/Mn-DSAzymes + H_2O_2 (0.1 mM), and Cu/Mn-DSAzymes + H_2O_2 (0.1 mM) + NIR-II groups, respectively. The irradiation group was exposed to a 1064 nm laser. On days 0, 3, 5, 7, and 9, the wound sites were measured to calculate the degree of wound healing. The body weights of mice were recorded for 9 days. On day 9, the wound and surrounding tissues were harvested, fixed with a 10% formaldehyde solution, dehydrated, embedded in paraffin, and sectioned for H&E or Masson's trichrome staining, revealing histopathological characteristics of the wounds treated with different groups. Wound tissues treated with different groups were collected on day 9, and the immunofluorescent staining of CD86, CD206, and CD31 was analyzed.

Statistical analysis. Statistical significance was assessed using a one-way ANOVA analysis on SPSS 16.0 software. The difference was statistically significant if the probability value was less than 0.05 ($p < 0.05$). Mean value and standard deviation (SD) were calculated for triplicate experiments. All data are presented as mean ± SD.
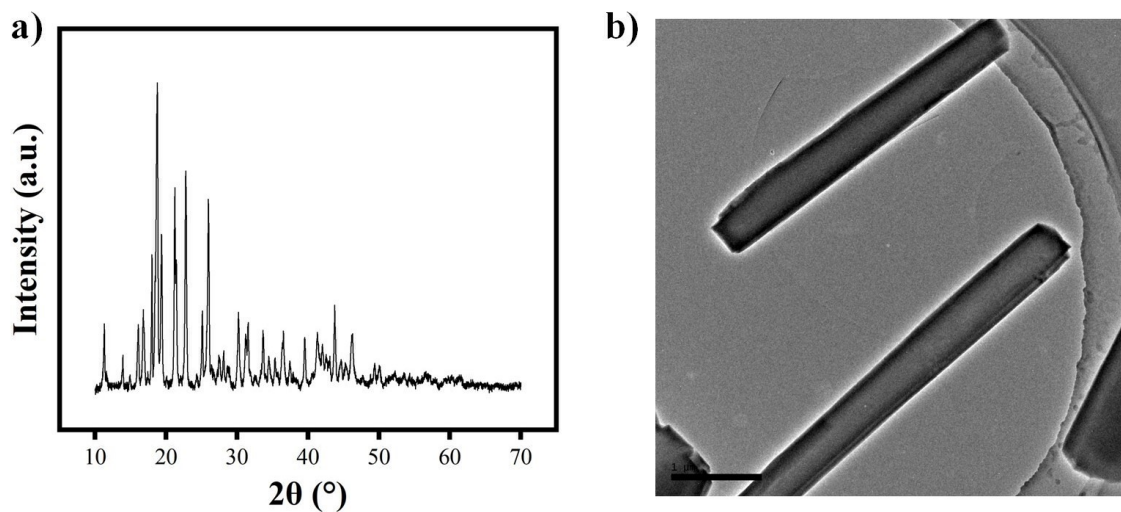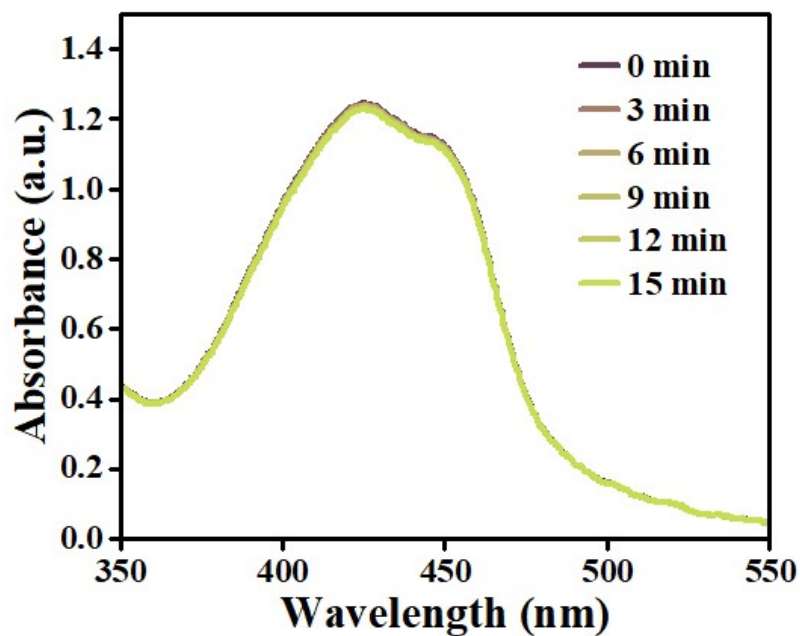
**Figure S1.** (a) XRD pattern and (b) TEM image of CuMn-BTC MOFs precursors.

CAT-like activity

$$H_2O_2 \xrightarrow{\text{Cu/Mn}-\text{DSAzymes}} O_2 + H_2O$$

OXD-like activity
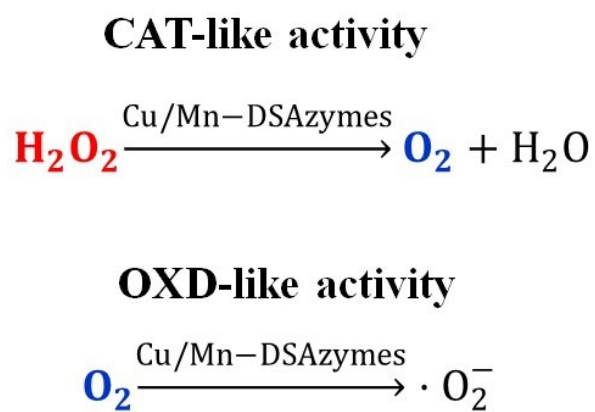
$$O_2 \xrightarrow{\text{Cu/Mn}-\text{DSAzymes}} \cdot O_2^-$$
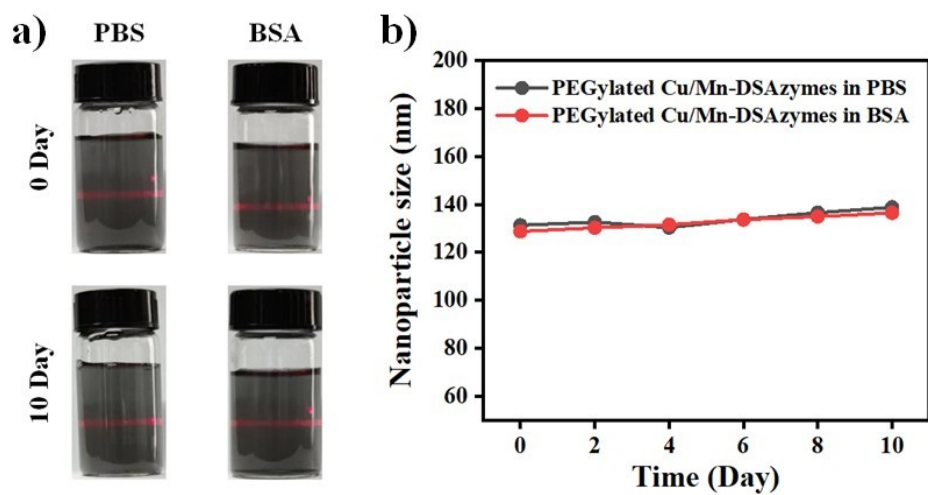
Figure S2. The reaction equation of dual enzymes mediated by Cu/Mn-DSAzymes.
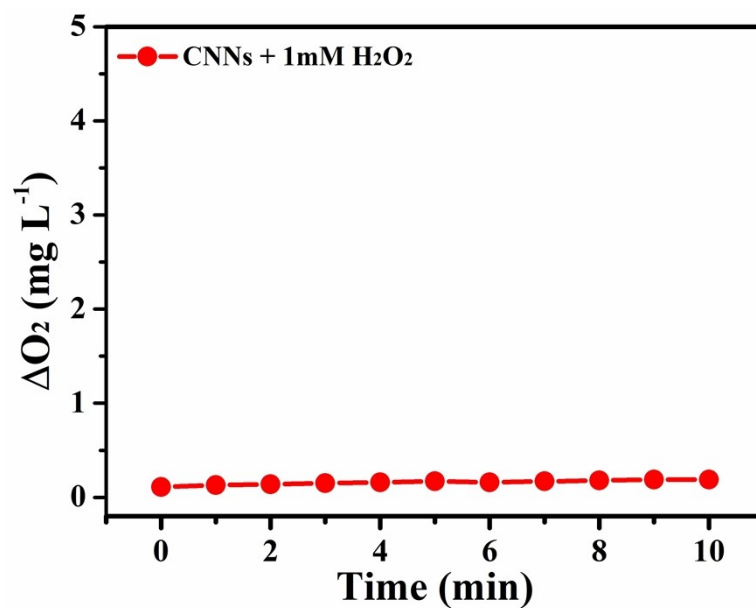
Figure S3. The O_2 generation from the decomposition of H_2O_2 through CNNs.

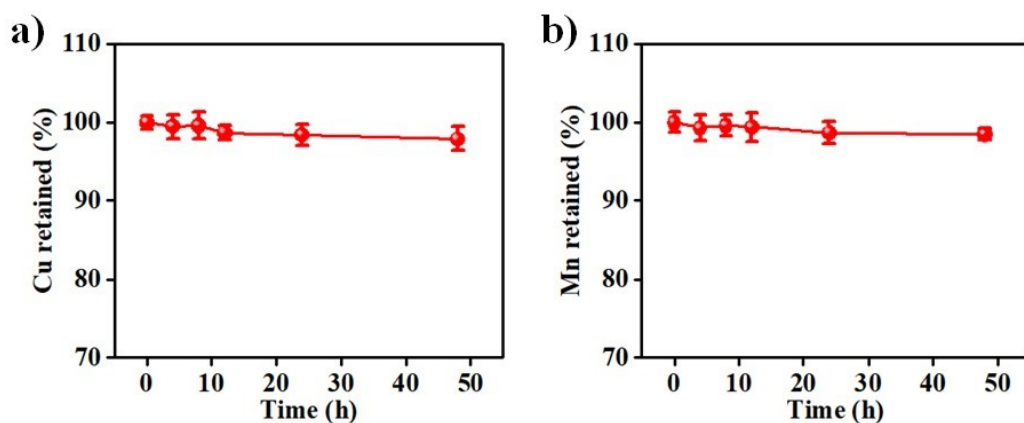**Figure S4.** Depletion of DPBF owing to $\cdot O_2^-$ production in the presence of CNNs and H_2O_2.
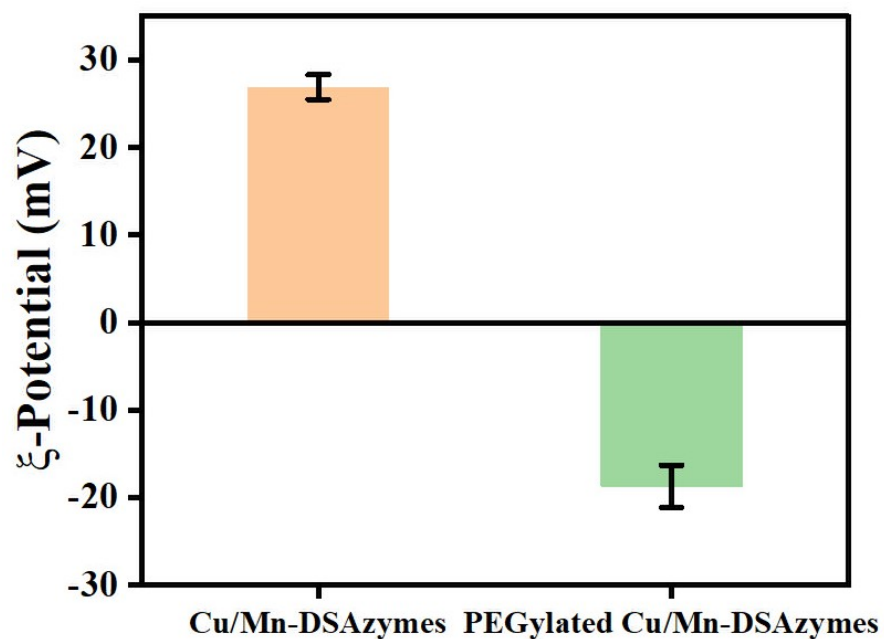
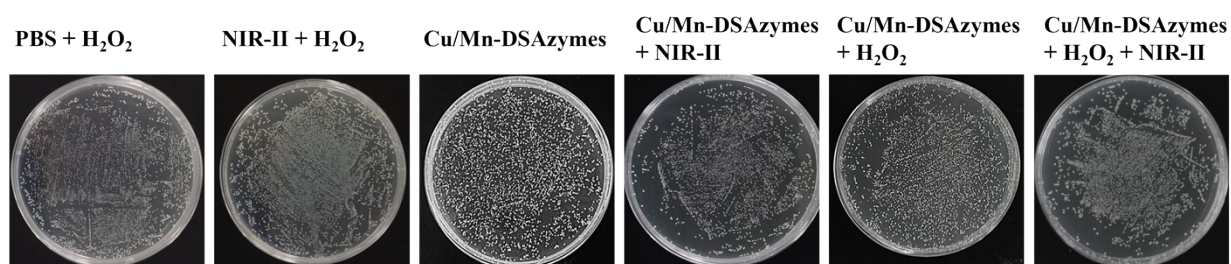**Figure S5.** Zeta potential ζ of PEGylated Cu/Mn-DSAzymes and Cu/Mn-DSAzymes.

Figure S6. (a) Photos of PEGylated Cu/Mn-DSAzymes dispersed in BSA and PBS after 10 days, respectively. (b) The nanoparticle size of PEGylated Cu/Mn-DSAzymes in BSA and PBS for 10 days, respectively.

Figure S7. The stability of (a) Cu and (b) Mn of Cu/Mn-DSAzymes in PBS.

Figure S8. Pictures of bacterial colony collected from MRSA-infected wounds before (day 1) treatment.
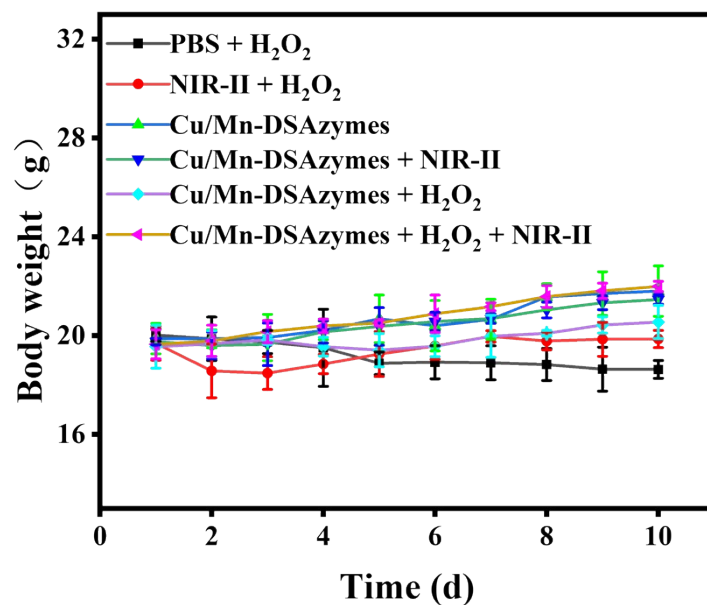
Figure S9. Changes in the mice body weights during the therapy. (n=5, mean ± SD)